Chapter

Review of Cervix Cancer Classification Using Radiomics on Diffusion-Weighted Imaging

Souha Aouadi, Nadin Mohamed, Jude Aloudeh, Mohamed Zeid, Othmane Bouhali, Rabih Hammoud, Noora Al-Hammadi and Tarraf Torfeh

Abstract

Magnetic Resonance Imaging (MRI) is one of the most used imaging modalities for the identification and quantification of various types of cancers. MRI image analysis is mostly conducted by experts relying on the visual interpretation of the images and some basic semiquantitative parameters. However, it is well known that additional clinical information is available in these images and can be harvested using the field of radiomics. This consists of the extraction of complex unexplored features from these images that can provide underlying functions in disease process. In this paper, we provide a review of the application of radiomics to extract relevant information from MRI Diffusion Weighted Imaging (DWI) for the classification of cervix cancer. The main research findings are the presentation of the state of the art of this application with the description of its main steps and related challenges.

Keywords: diffusion-weighted imaging, cervix cancer, tumor classification, machine learning, radiomics

1. Introduction

Cervical cancer (CC) has been determined to be the fourth leading cancer-induced cause of death in developed countries, and the second most common cause of death (due to cancer) in developing countries. It is also the second most occurring form of cancer among women [1]. Although, CC incidence is decreasing, thanks to human papillomavirus screening and vaccination programs, it remains a major health issue with around 604,000 new cases worldwide per year and more than 340,000 deaths per year [2, 3].

Treatment options for CC can be used separately or combined, and the choice of treatment methods depend on various prognostic risk factors including FIGO (Federation of Gynecology and Obstetrics) stage, histology, tumor volume, lymph node metastasis (LNM), and single-gene markers [4]. There are five main treatment methods that can be utilized for CC [5]. The first treatment option is surgery that

ranges from conization to total hysterectomies. Surgery is the gold standard for the treatment of early-stage CC (FIGO 1A1 IIA2). Other methods of treatment include external beam radiation therapy, which is often used with chemotherapy to target locally advanced CC (FIGO stage IIB IVA). In many cases, this is followed by internal beam radiation therapy (brachytherapy). Finally, immunotherapy and targeted therapy that have recently made some progress currently represent two clinical options for treating advanced recurrent CC. Despite the available treatment regiments, the 5-year overall survival is only 66% with considerable differences according to tumor classification [6]. The classification of CC in terms of tumor stage, grade, and histological type is of great importance in the clinical decision-making.

Medical images are increasingly used for diagnostic, therapy planning, and follow-up purposes by clinicians, thanks to the digitization of the information generated during a clinical routine. Moreover, visual interpretation of the images is moving towards a new type of radiology that integrates quantitative data (radiomics) extracted from the images [7]. Radiomics can be used to predict clinical information from medical images. The clinical information could be prognostic information (such as grade, stage, subtype, ...), a follow-up of pathological condition (such as tumor growth), or an assessment of treatment efficacy (such as patient survival) [8–10]. Furthermore, radiomics could be used to predict or decode hidden genetic and molecular traits for decision support [11–13].

Although several medical imaging modalities are available, MRI has become the modality of choice for the detection and quantification of various cancers due to its capability of acquiring excellent soft tissue contrast and functional images. As such, DWI, which allows for noninvasive analysis of tissues based on the random translational molecular motion of water molecules, presents various advantages for the characterization of the tumor and the understanding of its biology [14].

The purpose of this review is to present diffusion-weighted derived radiomics and their application for the classification of cervix cancer. The research findings represent the state of the art in the application of radiomics to the specific task of cervix cancer classification. A special focus was on the use of diffusion-weighted imaging and derived parameters. The feasibility of this task was demonstrated with a literature review of over 18 papers on the subject that were published in the last ten years. Furthermore, other findings of this review paper were the analysis of different challenges facing this application. Section 2 presents the physics of DWI and its major parameters and models are described. Section 3 gives a summary of the radiomics workflow. The description of the CC classification is given in section 4. Finally, we discuss the challenges for the use of radiomics in particular those based on DWI and possible future directions to move toward their application in clinical practice.

2. Physics of diffusion-weighted imaging

DWI measures the diffusion of water molecules within cellular tissues [15]. Diffusion stands for the random movement of molecules such as water within tissues propelled by thermal energy. DWI is achieved by applying diffusion sensitization gradients on either side of the 180° refocusing pulse of a spin echo sequence. The contrast of DWI is a result of the variance in the water molecules mobility in different regions [16]. This makes DWI sensitive to smaller abnormalities in tissue; hence, it is able to provide a more detailed characterization of the tissue [15].

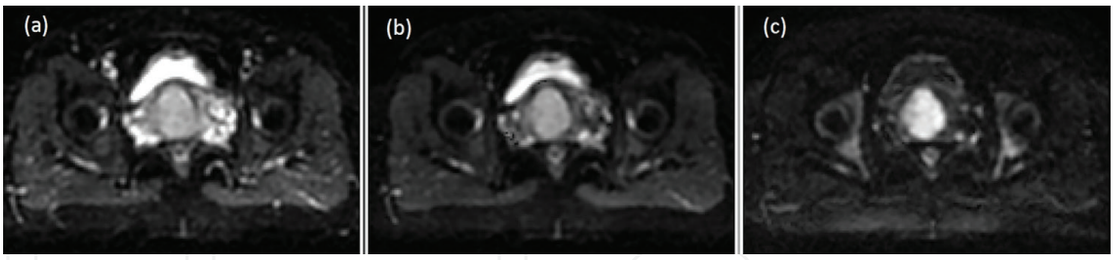

Figure 1.
(a) b = 0 no diffusion weighting. Image equivalent to T2 weighted image. The bladder is consequently brighter than the cervix tumor, (b) b = 100 intermediately diffusion-weighted image, and (c) b = 1000 strongly diffusion-weighted image. The cervix tumor is brighter compared to the bladder.

In a DWI sequence, the parameter "b-value" measures the degree of diffusion and is expressed in s/mm^2.The "b-value" is proportional to the square of the amplitude and duration of the gradient applied. The choice of b-values is crucial for the acquisition of DWI; **Figure 1** demonstrates how the "b-value" impacts the acquisition and in particular the tumor contrast. It depends on the anatomical site of the tumor as well as the model chosen for quantitative analysis. DWI models include mono-exponential model, intravoxel incoherent motion (IVIM), the Kurtosis model, and the stretched exponential model. These models vary depending on the perfusion and diffusion information that are considered.

The mono-exponential model is the simplest and most used for the analysis of DWI. It assumes a mono-exponential decay of the signal S with increasing b-values [16],

$$S = S_0 e^{-ADC\,b} \tag{1}$$

The ADC parameter describes the water diffusion in the tissue when derived from high b-values (> 200 s/mm2) and describes perfusion information when derived from low b-values (0 – 50 s/mm2). However, when it is acquired from a mixture of low and high b-values, diffusion and perfusion effects are incorporated.

In the IVIM model, the signal decay is modeled using a bi-exponential function, where the diffusion and perfusion parameters are included separately,

$$S = S_0\left(fe^{-D^*\cdot b} + \left(1-f\right)e^{-D\cdot b}\right) \tag{2}$$

f and D^* are the perfusion fraction (of the received signal) and the pseudo-diffusion coefficient (the diffusion caused by flowing blood), respectively, and D is the diffusion coefficient (clear of perfusion effects). In general, the IVIM model can produce the decayed signal of DWI more accurately [16].

The Kurtosis model is a corrected model of the previous two models, which considers the non-Gaussian diffusion behavior by an extra fit parameter, which is the kurtosis fit parameter K. The mono-exponential and IVIM models assume an isotropic Gaussian diffusion which is not always the case due to the interactions of the water molecules with micro components such as cell structures. The parameter K is complementary to the perfusion and diffusion parameters found in the mono-exponential and IVIM models, and D_K is the kurtosis-corrected diffusion coefficient.

$$S = S_0 e^{-bD_K + \frac{1}{6}b^2 D_K^2 K} \tag{3}$$

The kurtosis model requires obtaining very high b-values that should exceed 1000 s/mm^2.

Finally, the stretched exponential model has the equation,

$$S = S_0 e^{-(bDDC)^{\alpha}} \tag{4}$$

where α is the stretching parameter that describes the non-mono-exponential decay curves, and it lies between 0 and 1, and DDC is the distributed diffusion coefficient [17].

For the models based on both perfusion and diffusion information, a range of low b-values and high b-values are needed. For a voxel-by-voxel analysis of DWI, given very high b-values, the signals could be impacted by a high level of noise. In order to select the optimal b-values for a specific model and a specific anatomical site, a careful assessment of the signal decay curves is necessary [16].

The biological and physiological interpretation of the measurements that are extracted from DWI using a given model is not straightforward. In the literature, for cervix cancer, the mono-exponential model was mainly used with the interpretation of ADC values [18–28]. For instance, it was shown that the value of ADC for CC was lower than the value of normal cervix tissue (Chen et al. [15], McVeigh et al. [29], Naganawa et al. [20]). This reduction is expected to be due to hypercellularity within malignant tissues. These studies also determined that the completion of chemoradiotherapy resulted in increased ADC values, which could be explained by the removal of hypercellular tumoral tissues as well as the presence of edema, hyaline degeneration, and granulation tissue in the cervix post-therapy.

The impact of the choice of DWI models in differentiating between subtypes and grades of cervical tumors was studied by Winfield et al. [17]. The authors demonstrated that ADC alone was sufficient to predict tumor grade whereas the non-mono-exponential models (2), (3), and (4) provided a better characterization of tumor histological type. Therefore, Winfield et al. [17] concluded that the non-mono-exponential model parameters described different aspects of the tumor microstructure.

The following section describes the steps leading to the implementation of radiomics analysis for the prediction of prognosis factors.

3. Radiomic workflow

Radiomics is an emerging research field, where medical images are converted automatically into large number of quantitative features (radiomic features) that can be used for the characterization of tumor phenotypes [11]. Several oncological studies showed that radiomics are significantly associated with various biological properties of the tumor ranging from genetic aspects to tumor grading or staging and also to the prediction of the response to treatment [30–35]. The radiomic analysis workflow is composed of five steps as seen in **Figure 2**.

The first step in the radiomics workflow is the selection of the images. MRI, which offers high contrast and additional functional characterization of the soft tissues, represents the method of choice for radiomics calculation. However, MRI radiomics have not been investigated extensively in comparison to popular modalities, such as CT and PET [36].

The tumor is conventionally delineated manually by the radiation oncologist during treatment planning, which is not only time-consuming but also a source of

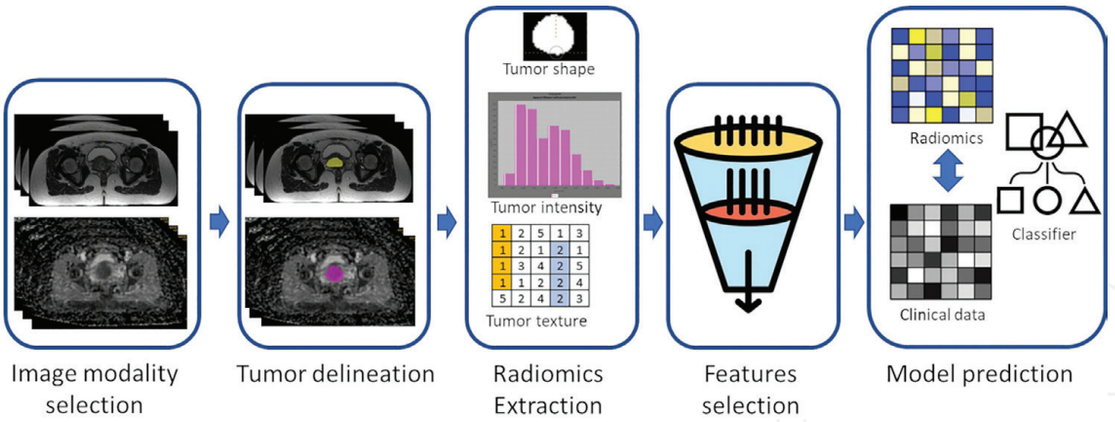

Figure 2.
The five steps of MRI-based radiomics workflow for cervical cancer. It includes the selection of the images to be used, the delineation of the tumor, the extraction and selection of the radiomics features, and finally the prediction of given clinical data.

interobserver variations. Automatic contouring of clinical target volume (CTV) and OARs has been clinically applied using atlas-based and model-based segmentation methods, which are now part of commercial radiotherapy planning devices. However, the automatic segmentation of the gross tumor volume (GTV) represents a difficult task and has no clinical applications so far. To the best of our knowledge, there is only one recent study that relies on deep learning for automatic segmentation of the GTV in CC from DWI [37].

Most frequently, open source software (such as LIFEx [38], MITK [39], PyRadiomics [13], or CERR [40]) or commercial ones (such as TexRAD [41]) is used to extract the radiomics features from the GTV. Three types of imaging features could be identified: shape, first order, and textural. Shape features describe the 3D geometric properties of the tumor while the first order features describe tumor intensity distribution. Texture features, which describe the intra-tumor heterogeneity, could be extracted from the gray level co-occurrence, gray level run length, gray level size zone, neighboring gray tone difference, and gray level dependence matrices. An image processing such as wavelet decomposition could be performed prior to the calculation of the first-order statistics and the textural features, which gives supplementary features.

Finally, the last two stages of the radiomics workflow constitute the machine learning model (MLM). Many radiomic features could be extracted from images. However, some features could be simply noise or correlated to each other. Therefore, it is important to perform feature selection to consider the most useful and unique features, which increases the MLM performance and reduces the computation time of the classifier. There are three types of feature selection techniques: filter, wrapper, and embedded methods [42]. Filter methods are independent approaches while wrapper and embedded methods are classifier-dependent approaches. Filter methods are computationally efficient and have high generalizability and scalability. Filter methods can be supervised or unsupervised depending on the use of the targeted labels. Supervised filters can be categorized into univariate and multivariate methods. Univariate methods perform ranking of individual features according to specific statistical criteria without considering the interrelationship between features and select the N top-ranked features. Multivariate techniques consider dependency between features. Unsupervised filter methods are based on dimensionally reduction algorithm and do not require information about the targeted labels [43].

Feature selection type	Learning type	Descriptive statistics	Algorithm name
Filter	Supervised	Univariate	Wilcoxon rank, ANOVA-F, Mutual information [44]
Filter	Supervised	Multivariate	Minimum Redundancy, Maximum Relevance [45], ReliefF [46]
Filter	Unsupervised	N/A	Principal Component Analysis [43], Independent Component Analysis [43]
Wrapper	Supervised	N/A	Forward Selection [42], Bi-Directional elimination [42]
Embedded Methods	Supervised	N/A	Elastic net regression, Lasso regression [47]

Table 1.
Examples of feature selection algorithms.

Wrapper methods rely on a specific machine learning model that is fitted to data to find the optimal features. The best combination of features according to an evaluation criterion is selected. Wrapper methods suffer from high computation time for dataset with many features and a high chance of overfitting. Two techniques under wrapper methods are forward selection (FS) and bi-directional elimination (BDE) [42].

In embedded methods, the optimal subset of features is searched while building a classifier. Embedded methods are computationally efficient in comparison to wrappers but use a strict classifier assumption and hence lack generalizability. **Table 1** summarizes the feature selection algorithms type cited above.

Following the filter or the wrapper features selection, the remaining, most significant features are then fed into a machine learning classifier that can determine the probabilities of the tumor being in the different categories. This classifying procedure ends when the classifier of choice is trained on appropriate training data set with the resulting performance tested on validation and testing sets. The validation set is used to optimize the parameters of the model. The testing set is used to evaluate the performance of the trained/optimized model on data that was never used for training or validation.

4. Application of DWI-based radiomics to the classification of CC

The classification of CC consists of the determination of the histological type, the grade, and the stage of the tumor. The classification is important for the prognosis of the disease and can provide information that can be used to predict future patient outcomes. A summary of the studies, published in the last ten years for the classification of CC from DWI using radiomics analysis, is given in **Table 2**. For each publication, the authors, the year of publication, the type of the study, the number of patients, the main conclusion, the evaluation metrics, the radiomic features, the machine learning model (MLM) and statistical analysis done, and the modality used are given. In these studies, multiparametric MRI (T1-weighted MRI (T1), T2-weighted MRI (T2), DWI, DCE-MRI), a single sequence, or derived images from the models of DWI were investigated.

Authors	Year	T	NP	Main Conclusion	Evaluation metrics	Radiomic features	MLM and statistical analysis	MOD
Zhang et al. [48]	2021	p	76	Differentiation of cervical cancer subtypes and SCC grades possible with DKI features	AUC	First-order texture features	Mann-Whitney U test and ROC curve for features selection, multivariate logistic regression analysis	DKI, DWI
Wei Wang et al. [49]	2021	R	96	Promising methods to differentiate between AC and SCC	AUC, ACC, SE, SP	105 RF	Clustering and logistic regression	T1c, T2, ADC
Jajodia et al. [50]	2021	R	83	Prediction of FIGO stage in addition to recurrence, distant metastasis, lymph node metastasis is feasible	AUC, Cohen's Kappa	24 RF were selected (first-order, texture, wavelet)	k- nearest neighbors, regularized random forest	DWI, ADC
Mandi Wang et al. [51]	2020	R	95	It is possible to discriminate histological subtypes, tumor grades, FIGO stages, and nodal status	AUC	First-order texture features	Elastic net for features selection, multivariable support vector machine model for prediction	T2, T1c, ADC
Yamada et al. [52]	2020	R	58	RF model helps in differentiating grade and stage of the tumor better than adc values	AUC	45 RF (Shape, histogram-based, textural)	Random forest	ADC, DWI
Li et al. [53]	2020	R	63	The ADC values showed a significant difference in grade prediction	AUC, ACC, SE, SP	Average values of ADC and T2 in the tumor	t-test, Wilcoxon signed-rank test, and the chi-square test used for comparison	T2, DWI ADC
Xiao et al. [54]	2020	R	233	A radiomics nomogram can predict the LNM in patients with early-stage CC	AUC, SE, SP, C-index, Hosmer–Lemeshow test	first-order, shape-based, textural, and wavelet RF	Feature selection by LASSO, multivariate logistic regression analysis	T1, T2, T1c, DWI, ADC
Umutlu et al. [55]	2020	R	30	The prediction of N and M stages based on radiomic analyses is feasible	AUC, SE, SP	45 features from each modality (first-order, GLCM, GLRLM)	Prediction of M-stage (N-stage) using SVM (RBF-SVM) with SVM-RFE (MIFS) as feature selection	F-FDG PET/MR, ADC
Kitajima et al. [56]	2020	R	62	pelvic MRI provides reliable imaging findings for T staging	AUC, ACC, SP, SE, PPV, NPV	Shape, intensity, and texture features	The stage is determined from MRI by experts based on [57]	T2, T1, T1c, DWI

Authors	Year	T	NP	Main Conclusion	Evaluation metrics	Radiomic features	MLM and statistical analysis	MOD
Liu et al.[14]	2019	P	160	Radiomics analysis of ADC map helps with differentiating tumor grade	Misclassification error	208 RF (histogram-based, textural, LoG)	Lasso regression	T2, ADC, DWI
Wu et al. [58]	2019	R	189	MRI-based radiomics analysis may predict lymph nodes metastasis status	AUC, SE, SP	1299 RF (shape, intensity, texture, wavelet, LOG) features from intra- and peri-tumoral tissues	Feature selection by LASSO regression, prediction by SVM	T2, DWI, ADC
Ciolina et al. [59]	2019	R	28	RF may differentiate histological tumor types	SE, SP	Mean, skewness	Unpaired t-test	T2, ADC
Panying Wang et al. [60]	2018	R	50	Differentiating grade and stage is feasible	AUC, ACC, SE, SP	Mean values of ADC, D_{app} K_{app}	One way ANOVA test, Pearson's correlation coefficient	DWI, DKI, ADC, D_{app}, K_{app}
Wu et al. [61]	2018	R	56	the radiomics analysis of multiparametric MRI features allows for the discrimination of tumor grade of CC.	ROC, AUC, ACC, SP, SE, PPV, NPV	histogram, first-order texture, GLCM, RLM	Mann–Whitney U-test, PCA, Logistic regression	T2, DWI, DCE
Becker et al. [62]	2017	P	23	GLCM features predictive of grade, histogram features predictive of stage	Correlation and statistical significance	Histogram-based and GLCM features	Spearman, Kruskal-Wallis for the assessment of correlation to clinical data	DWI, ADC
Duan et al. [63]	2016	R	116	The staging of neuroendocrine carcinoma (NEC) in uterine cervix can be reliably done with MRI	AUC, SE, SP	Use of cutoff level that maximizes sum of SE and SP	Fisher and $\chi 2$ test for features comparison. Staging done by experts based on [57]	T2, DWI, ADC
Miccò et al. [64]	2014	R	49	There is a correlation between imaging parameters (ADC_{mean}) and histopathological prognostic factors (grade, stage, and subtype)	Correlation and statistical significance	Mean ADC	Wilcoxon Rank Sum test	DWI, T1c, PET/ CT

Authors	Year	T	NP	Main Conclusion	Evaluation metrics	Radiomic features	MLM and statistical analysis	MOD
Downey et al. [65]	2013	P	60	RF may differentiate cervical tumors according to their histologic characteristic (subtype and grade)	Statistical significance	Histogram-based RF	independent samples Student t-test for the comparison of RF differences	T2, DWI, ADC

For each study, the year of publication, the type (T), the number of patients (NP), the main conclusion, the evaluation metrics, the radiomic features, the machine learning model (MLM), and statistical analysis done and the modality (MOD) used are given.
Glossary: T, study type; R, retrospective; P, prospective; NP, number of patients; CAC, cervical adenocarcinoma; SCC, squamous cell carcinoma respectively; AUC, the area under the roc curve; SP, specificity; SE, sensitivity; ACC, accuracy; PPV, positive predictive value; NPV, negative predictive value; RF, radiomics features; LoG, laplacian of gaussian; GLCM, grey level co-occurrence matrix; RLM, Run Length Matrix features; SVM, support vector machine; SVM-RFE, Support vector machine recursive feature elimination; MIFS, mutual information feature selection; MOD, type of MRI used; T2, T2 weighted MRI; T1, T1 weighted MRI; T1c, contrast-enhanced T1; DWI, diffusion weighted images; ADC, apparent diffusion coefficient; DKI, Diffusdon kurtosis imaging; D_{app}, apparent coefficient; K_{app}, the apparent kurtosis; DCE, dynamic contrast-enhanced MRI.

Table 2.
Summary of the papers found for the classification of cervical cancer from DWI using radiomics analysis.

4.1 Prediction of histological type

Histopathology is a cornerstone in the diagnosis of cervical cancer. Squamous cell carcinoma is the predominant histological type with a 75% rate of all cervical cancers. Adenocarcinoma and adenosquamous cell carcinoma represent 10–15%, and other or unspecified histology represents the remaining 10–15% [66]. The histological type was found to be an important independent prognostic factor in CC based on a record of 30,989 cases between 1973 and 2002 in Ref. [66]. This study reported that small cell carcinoma and adenocarcinomas were associated with poorer survival and this emphasized the need to identify women at risk early [66].

Several studies have been done on the application of texture analysis in the prediction of histological type for CC. Zhang et al. [48] proposed a model based on first-order texture features extracted from functional maps of DWI; it gave accurate differentiation between cervical squamous cell cancer (SCC) and cervical adenocarcinoma (CAC) with an AUC=0.932. Wang et al. [49, 51] investigated multiparametric MRI including ADC. They demonstrated better differentiation capability between SCC and CAC in comparison to each MRI sequence alone when using clustering and regression model of 105 RF or SVM; an AUC above 0.84 was reported. Ciolina et al. [59] were able to discriminate SCC and CAC based on texture analysis that used the mean and skewness values. Similarly, Downey et al. [65] demonstrated that histogram-positive skew was lower in CAC compared to SCC and this was assumed to reflect the glandular content of adenocarcinoma.

4.2 Prediction of tumor grade

Tumor grade is important information that helps oncologists decide on the treatment strategies. Cancer grading describes the cellular phenotype of the tumor in comparison to healthy cells. There are three grades of tumor cells: grade 1 (well differentiated), grade 2 (moderately differentiated), and grade 3 (poorly differentiated) from normal cells. Traditionally, the determination of the grade requires a biopsy: a sample of the cervix is taken and analyzed under a microscope. The treatment protocol differs from one grade to another, which is why grade identification is a crucial step in cancer treatment decisions [67, 68].

Several studies have been conducted on the prediction of cervix tumor grade from DWI [14, 48, 51, 52, 58, 60, 62, 64, 65] as described in **Table 2**. Liu et al. demonstrated that whole-tumor volumetric 3D radiomics analysis had a better performance than using the 2D center-slice of tumor in stratifying the histological grade of cervical cancer [14]. In 2020, a paper by Yamada et al. [52] studied the prediction of histologic grade based on ADC maps from 58 CC patients. A random forest model using textural features demonstrated a significantly larger AUC in comparison to ADC values for the prediction of high-grade cervical carcinoma. Hence, it was concluded that texture analysis of ADC maps could be used for pretreatment prognostication and optimal treatment selection in patients with cervical carcinoma in the future. However, validation of more patients is still necessary.

4.3 Prediction of tumor stage

The first staging system for cervical cancer has been developed by the FIGO in 1958 and since then several revisions have been issued [69]. The new FIGO system consists of five different stages [70] and provides better guidance on cancer

management. The staging of the tumor determines the actual extent of the disease in the body and anticipates response to treatment. It is crucial for the determination of the treatment strategy and the prediction of patient survival. Several studies have shown that cervical cancer has a five-year survival rate of 65% for FIGO stage II, 40% for FIGO stage III, and 15% for FIGO stage IV-A [71].

Many studies have been conducted on the prediction of cervix tumor stage from DWI alone or combined with other MR sequences [50–52, 54–56, 60–64] as summarized in **Table 2**. Lin et al. [72] investigated the application of histogram-based features that were computed on ADC for the differentiation of early-stage CC from normal cervix or cervical benign lesions; features were significantly different between both classes based on a prospective dataset of 73 patients. In their study, in which a dataset of 56 patients was investigated, Guan et al. [73] demonstrated that ADC first-order statistics (skewness, kurtosis, and entropy) and texture features derived from the grey-level co-occurrence matrix can be correlated significantly with the FIGO stages of CC.

5. Challenges

The use of DWI-based radiomics in the classification of CC has been shown to be effective. Many studies used DWI alone or in combination with other MRI sequences (such as T1 and T2) and image modalities (such as PET). DWI and derived maps were related to hypercellularity within malignant tissues as they describe the perfusion and diffusion phenomena in the tissues. Sophisticated radiomic analysis demonstrated better performance in comparison to the use of simple image values such as average intensities within the tumor. The application of radiomics was proven to enhance the performance of differentiating between different stages, grades, and histological types of CC. However, there are some challenges that still need to be overcome before the application in clinical practice. This section outlines some of the important challenges in utilizing radiomics in clinical diagnosis and prognosis.

5.1 DWI artifacts and the impact of image acquisition

DWI is obtained using rapid Echo-Planar Imaging (EPI). The challenge related to EPI sequences is that they are susceptible to geometric distortions, which arise in phase-encoding direction. System-related distortions come from the inhomogeneities of the static magnetic field and the nonlinearity of the gradient magnetic field while object-related distortions arise from susceptibility differences within the imaged patient. In addition to these issues, signal loss occurs and causes the quantification accuracy to decrease. Robust quantification of DWI-derived parameters is another important aspect that should be addressed. Noise and artifacts that accompany signals should be bounded within reasonable limits for the applied model (mono-exponential model, IVIM, and the Kurtosis model) [16].

In addition to image artifacts, the main challenge preventing the implementation of radiomics in routine practice is the lack of standardization of image acquisition protocols. The variance between data collection protocols, scanners, coils, and manufacturers can introduce a large variation of signal intensities and thus impact the stability of radiomic features. The robustness, reproducibility, and repeatability (defined in [74]) of derived radiomics are the criteria that need to be verified for different imaging protocols; some features may verify these criteria whereas others may

not. To the best of our knowledge, the robustness, reproducibility, and repeatability of radiomics features based on cervix DWI were not investigated.

5.2 Image segmentation

Most radiomics features are affected by tumor segmentation methods. When using manual or semiautomated contouring methods, radiomics may not be robust to intra and interobserver variations and this needs to be assessed so that only reproducible features are considered. Interobserver delineation variations offer better feature reproducibility in comparison to other variations in imaging protocols [75]. Baeßler et al. [76] demonstrated that using FLAIR imaging, specifically at high resolutions resulted in more robust radiomics features to intra and interobserver variability in comparison to T1 and T2 weighted images and hence can be reliably applied in future clinical studies. They concluded that fully automatic image segmentation is crucial to reduce the high inter and intraobserver variability and thus reduce the effect of subjective bias. However, automated segmentation is often developed for organ delineation and not for GTV.

5.3 Radiomics calculation

The standardization of radiomics calculation approaches is an essential step toward their clinical implementation. A prior image processing is needed. Image processing techniques are very important as they allow for standardization and verifiable reference points and; therefore, allow for results to be reproduced in the future. Usually, images are resampled into isotropic voxel sizes, and their intensities rescaled and discretized [77]. The optimal choice of image processing parameters, such as the bin width and bin size, in case of discretization influences the value of radiomics, and it is still an open question, especially in the case of MRI. Furthermore, the feature calculation methods can differ between studies, which makes challenging the reproduction of the results. The adherence to the Image Biomarker Standardization Initiative (IBSI) guidelines is recommended as it allows (a) establishing a nomenclature and definitions for commonly used radiomics features, (b) creating a radiomics imaging scheme to calculate features from images, (c) providing a set of reference values for verification and calibration of various software used, and (d) providing a set of reporting guidelines for studies dealing with radiomics analyses [77].

5.4 Prediction techniques

Although MRI-derived radiomics demonstrated predictive potential for different cancer sites, the variance between the prediction techniques precluded their generalizability and the collective interpretation of the data [78]. The performance of machine learning models is conditioned by the noncorrelation between their inputs. This makes the feature selection/reduction step crucial in the radiomics workflow. For this step, machine learning approaches or statistical methods are performed, after an analysis of reproducibility, to remove the correlated clusters, and finally, model fitting is done [79]. The prediction approach is not only sensitive to the parameters used to compute the radiomics but also to the size of the training and validation set. In most publications, the prediction models are based on a hundred subjects or fewer. This may result in over-fitting especially when a high number of features is used. Hence, particular care must be taken on the selected features to have reasonable conclusions.

The utilization of machine learning and deep learning methods in radiomics can allow for more personalized cancer treatments and more accurate prognoses. However, physicians in practice are hesitant to exploit such methods clinically because machine learning algorithms have long been known as "black boxes" as it is still unknown to data scientists the reasoning behind the model prediction [80].

6. Conclusion

The field of radiomics and its applications for cervix cancer is at a turning point. Over ten years of literature have given many proofs for the potential of the use of DWI-based features for cervix cancer classification. Nevertheless, the transition into clinical practice will not be possible unless various challenges are overcome.

Future research directions will consist of proposing in-house solutions for cervix cancer classification. A database will be built retrospectively by the collection of cervix cancer image data, tumor contours, and clinical information (grade, stage, and histology of the tumor). DWI-based radiomics and deep learning workflows will be implemented in-house for this task and compared.

Author details

Souha Aouadi[1*], Nadin Mohamed[2], Jude Aloudeh[2], Mohamed Zeid[2], Othmane Bouhali[3], Rabih Hammoud[1], Noora Al-Hammadi[1] and Tarraf Torfeh[1]

1 Department of Radiation Oncology, National Center for Cancer Care and Research, Hamad Medical Corporation, Doha, Qatar

2 Department of Electrical Engineering, Texas A and M University at Qatar, Doha, Qatar

3 Department of Science, Texas A&M University at Qatar, Doha, Qatar

*Address all correspondence to: saouadi@hamad.qa

References

[1] Arbyn M, Weiderpass E, Bruni L, de Sanjosé S, Saraiya M, Ferlay J, et al. Estimates of incidence and mortality of cervical cancer in 2018: A worldwide analysis. The Lancet Global Health. 2020;**8**:e191-e203

[2] Sung H, Ferlay J, Siegel RL, Laversanne M, Soerjomataram I, Jemal A, et al. Global Cancer Statistics 2020: GLOBOCAN Estimates of Incidence and Mortality Worldwide for 36 Cancers in 185 Countries. CA: A Cancer Journal for Clinicians. 2021;**71**:209-249

[3] Brisson M, Kim JJ, Canfell K, Drolet M, Gingras G, Burger EA, et al. Impact of HPV vaccination and cervical screening on cervical cancer elimination: A comparative modelling analysis in 78 low-income and lower-middle-income countries. Lancet. 2020;**395**:575-590

[4] Marth C, Landoni F, Mahner S, McCormack M, Gonzalez-Martin A, Colombo N. Cervical cancer: ESMO Clinical Practice Guidelines for diagnosis, treatment and follow-up. Annals of Oncology. 2017;**28**:72-83

[5] Cohen PA, Jhingran A, Oaknin A, Denny L. Cervical cancer. Lancet. 2019;**393**:169-182

[6] Manganaro L, Nicolino GM, Dolciami M, Martorana F, Stathis A, Colombo I, et al. Radiomics in cervical and endometrial cancer. The British Journal of Radiology. 2021;**94**:20201314

[7] Scapicchio C, Gabelloni M, Barucci A, Cioni D, Saba L, Neri E. A deep look into radiomics. La Radiologia Medica. 2021;**126**:1296-1311

[8] Alobaidli S, McQuaid S, South C, Prakash V, Evans P, Nisbet A. The role of texture analysis in imaging as an outcome predictor and potential tool in radiotherapy treatment planning. British Journal of Radiology. 2014;**87**:20140369

[9] Haralick RM, Shanmugam K, Dinstein I. Textural features for image classification. IEEE Transactions on Systems, Man, and Cybernetics. 1973;**SMC-3**:610-621

[10] Lee G, Lee HY, Park H, Schiebler ML, van Beek EJR, Ohno Y, et al. Radiomics and its emerging role in lung cancer research, imaging biomarkers and clinical management: State of the art. European Journal of Radiology. 2017;**86**:297-307

[11] Aerts HJWL, Velazquez ER, Leijenaar RTH, Parmar C, Grossmann P, Cavalho S, et al. Decoding tumour phenotype by noninvasive imaging using a quantitative radiomics approach. Nature Communication. 2014;**5**:4006

[12] Lambin P, Rios-Velazquez E, Leijenaar R, Carvalho S, van Stiphout RGPM, Granton P, et al. Radiomics: Extracting more information from medical images using advanced feature analysis. European Journal of Cancer. 2012;**48**:441-446

[13] van Griethuysen JJM, Fedorov A, Parmar C, Hosny A, Aucoin N, Narayan V, et al. Computational Radiomics System to Decode the Radiographic Phenotype. Cancer Research. 2017;**77**:e104-e107

[14] Liu Y, Zhang Y, Cheng R, Liu S, Qu F, Yin X, et al. Radiomics analysis of apparent diffusion coefficient in cervical cancer: A preliminary study on histological grade evaluation. Journal of Magnetic Resonance Imaging. 2019;**49**:280-290

[15] Chen J, Zhang Y, Liang B, Yang Z. The utility of diffusion-weighted MR imaging in cervical cancer. European Journal of Radiology. 2010;**74**:e101-e106

[16] Leibfarth S, Winter RM, Lyng H, Zips D, Thorwarth D. Potentials and challenges of diffusion-weighted magnetic resonance imaging in radiotherapy. Clinical Translation Radiation Oncology. 2018;**13**:29-37

[17] Winfield JM, Orton MR, Collins DJ, Ind TEJ, Attygalle A, Hazell S, et al. Separation of type and grade in cervical tumours using non-mono-exponential models of diffusion-weighted MRI. European Radiology. 2017;**27**:627-636

[18] Gladwish A, Milosevic M, Fyles A, Xie J, Halankar J, Metser U, et al. Association of apparent diffusion coefficient with disease recurrence in patients with locally advanced cervical cancer treated with radical chemotherapy and radiation therapy. Radiology. 2016;**279**:158-166

[19] Haack S, Tanderup K, Kallehauge JF, Mohamed S, Mohamed I, Lindegaard JC, Pedersen EM, Diffusion-weighted magnetic resonance imaging during radiotherapy of locally advanced cervical cancer – treatment response assessment using different segmentation methods. 2015

[20] Naganawa S, Sato C, Kumada H, Ishigaki T, Miura S, Takizawa O. Apparent diffusion coefficient in cervical cancer of the uterus: Comparison with the normal uterine cervix. European Radiology. 2005;**15**:71-78

[21] Daniel M, Andrzejewski P, Sturdza A, Majercakova K, Baltzer P, Pinker K, et al. Impact of hybrid PET/MR technology on multiparametric imaging and treatment response assessment of cervix cancer. Radiotherapy and Oncology. 2017;**125**:420-425

[22] Zhu L, Wang H, Zhu L, Meng J, Xu Y, Liu B, et al. Predictive and prognostic value of intravoxel incoherent motion (IVIM) MR imaging in patients with advanced cervical cancers undergoing concurrent chemo-radiotherapy. Scientific Reports. 2017;**7**:1-9

[23] Das S, Chandramohan A, Rami Reddy JK, Mukhopadhyay S, Kumar RM, Isiah R, et al. Role of conventional and diffusion weighted MRI in predicting treatment response after low dose radiation and chemotherapy in locally advanced carcinoma cervix. Radiotherapy and Oncology. 2015;**117**:288-293

[24] Schreuder SM, Lensing R, Stoker J, Bipat S. Monitoring treatment response in patients undergoing chemoradiotherapy for locally advanced uterine cervical cancer by additional diffusion-weighted imaging: A systematic review. Journal of Magnetic Resonance Imaging. 2015;**42**:572-594

[25] Schernberg A, Balleyguier C, Dumas I, Gouy S, Escande A, Bentivegna E, et al. Diffusion-weighted MRI in image-guided adaptive brachytherapy: Tumor delineation feasibility study and comparison with GEC-ESTRO guidelines. Brachytherapy. 2017;**16**:956-963

[26] Heo SH, Shin SS, Kim JW, Lim HS, Jeong YY, Kang WD, et al. Pre-treatment diffusion-weighted MR imaging for predicting tumor recurrence in uterine cervical cancer treated with concurrent chemoradiation: Value of histogram analysis of apparent diffusion coefficients. Korean Journal of Radiology. 2013;**14**:616

[27] Onal C, Erbay G, Guler OC. Treatment response evaluation using

the mean apparent diffusion coefficient in cervical cancer patients treated with definitive chemoradiotherapy. Journal of Magnetic Resonance Imaging. 2016;**44**:1010-1019

[28] Marconi DG, Fregnani JHTG, Rossini RR, Netto AKBJ, Lucchesi FR, Tsunoda AT, et al. Pre-treatment MRI minimum apparent diffusion coefficient value is a potential prognostic imaging biomarker in cervical cancer patients treated with definitive chemoradiation. BMC Cancer. 2016;**16**:556

[29] McVeigh PZ, Syed AM, Milosevic M, Fyles A, Haider MA. Diffusion-weighted MRI in cervical cancer. European Radiology. 2008;**18**:1058-1064

[30] Sun R, Limkin EJ, Vakalopoulou M, Dercle L, Champiat S, Han SR, et al. A radiomics approach to assess tumour-infiltrating CD8 cells and response to anti-PD-1 or anti-PD-L1 immunotherapy: An imaging biomarker, retrospective multicohort study. The Lancet Oncology. 2018;**19**:1180-1191

[31] Delzell DAP, Magnuson S, Peter T, Smith M, Smith BJ. Machine learning and feature selection methods for disease classification with application to lung cancer screening image data. Frontiers in Oncology. 2019;**9**:1-8

[32] Shi L, He Y, Yuan Z, Benedict S, Valicenti R, Qiu J, et al. Radiomics for response and outcome assessment for non-small cell lung cancer. Technology in Cancer Research & Treatment. 2018;**17**:1-14

[33] Liang C, Huang Y, He L, Chen X, Ma Z, Dong D, et al. The development and validation of a CT-based radiomics signature for the preoperative discrimination of stage I-II and stage III-IV colorectal cancer. Oncotarget. 2016;**7**:31401-31412

[34] Parmar C, Grossmann P, Bussink J, Lambin P, Aerts HJWL. Machine learning methods for quantitative radiomic biomarkers. Scientific Reports. 2015;**5**:13087

[35] Parmar C, Grossmann P, Rietveld D, Rietbergen MM, Lambin P, Aerts HJWL. Radiomic machine-learning classifiers for prognostic biomarkers of head and neck cancer. Frontiers in Oncology. 2015;**5**:272

[36] Schick U, Lucia F, Dissaux G, Visvikis D, Badic B, Masson I, et al. MRI-derived radiomics: Methodology and clinical applications in the field of pelvic oncology. British Journal of Radiology. 2019;**92**:20190105

[37] Kano Y, Ikushima H, Sasaki M, Haga A. Automatic contour segmentation of cervical cancer using artificial intelligence. Journal of Radiation Research. 2021;**62**:934-944

[38] Nioche C, Orlhac F, Boughdad S, Reuze S, Goya-Outi J, Robert C, et al. Lifex: A freeware for radiomic feature calculation in multimodality imaging to accelerate advances in the characterization of tumor heterogeneity. Cancer Research. 2018;**78**:4786-4789

[39] Götz M, Nolden M, Maier-Hein K. MITK Phenotyping: An open-source toolchain for image-based personalized medicine with radiomics. Radiotherapy and Oncology. 2019;**131**:108-111

[40] Apte AP, Iyer A, Crispin-Ortuzar M, Pandya R, van Dijk LV, Spezi E, et al. Technical Note: Extension of CERR for computational radiomics: A comprehensive MATLAB platform for reproducible radiomics research. Medical Physics. 2018;**45**:3713-3720

[41] Ytre-Hauge S, Dybvik JA, Lundervold A, Salvesen ØO, Krakstad C,

Fasmer KE, et al. Preoperative tumor texture analysis on MRI predicts high-risk disease and reduced survival in endometrial cancer. Journal of Magnetic Resonance Imaging. 2018;**48**:1637-1647

[42] Wan C. Feature Selection Paradigms Hierarchical Feature. Cham: Springer; 2019. pp. 17-23

[43] Hira ZM, Gillies DF. A review of feature selection and feature extraction methods applied on microarray data. Advances in Bioinformatics. 2015;**2015**:1-13

[44] Vergara JR, Estévez PA. A review of feature selection methods based on mutual information. Neural Computing and Applications. 2014;**24**:175-186

[45] Radovic M, Ghalwash M, Filipovic N, Obradovic Z. Minimum redundancy maximum relevance feature selection approach for temporal gene expression data. BMC Bioinformatics. 2017;**18**:9

[46] Urbanowicz RJ, Meeker M, La Cava W, Olson RS, Moore JH. Relief-based feature selection: Introduction and review. Journal of Biomedical Informatics. 2018;**85**:189-203

[47] R Core. University of T. Tibshirani, Regression Shrinkage and Selection via the Lasso. Journal of Statistics. 2018;**58**:267-288

[48] Zhang Q, Yu X, Ouyang H, Zhang J, Chen S, Xie L, et al. Whole-tumor texture model based on diffusion kurtosis imaging for assessing cervical cancer: A preliminary study. European Radiology. 2021;**31**:5576-5585

[49] Wang W, Jiao Y, Zhang L, Fu C, Zhu X, Wang Q, et al. Multiparametric MRI-based radiomics analysis: Differentiation of subtypes of cervical cancer in the early stage. Acta Radiology. 2022;**63**:847-856

[50] Jajodia A, Gupta A, Prosch H, Mayerhoefer M, Mitra S, Pasricha S, et al. Combination of radiomics and machine learning with diffusion-weighted MR imaging for clinical outcome prognostication in cervical cancer. Tomography. 2021;**7**:344-357

[51] Wang M, Perucho JAU, Tse KY, Chu MMY, Ip P, Lee EYP. MRI texture features differentiate clinicopathological characteristics of cervical carcinoma. European Radiology. 2020;**30**:5384-5391

[52] Yamada I, Oshima N, Miyasaka N, Wakana K, Wakabayashi A, Sakamoto J, et al. Texture analysis of apparent diffusion coefficient maps in cervical carcinoma: Correlation with histopathologic findings and prognosis. Radiol. Imaging Cancer. 2020;**2**:e190085

[53] Li S, Liu J, Zhang F, Yang M, Zhang Z, Liu J, et al. Novel T2 mapping for evaluating cervical cancer features by providing quantitative T2 maps and synthetic morphologic images: A Preliminary Study. Journal of Magnetic Resonance Imaging. 2020;**52**:1859-1869

[54] Xiao M, Ma F, Li Y, Li Y, Li M, Zhang G, et al. Multiparametric MRI-based radiomics nomogram for predicting lymph node metastasis in early-stage cervical cancer. Journal of Magnetic Resonance Imaging. 2020;**52**:885-896

[55] Umutlu L, Nensa F, Demircioglu A, Antoch G, Herrmann K, Forsting M, et al. Radiomics analysis of multiparametric PET/MRI for N- and M-staging in patients with primary cervical cancer. RöFo - Fortschritte Auf Dem Gebiet Der Röntgenstrahlen Und Der Bildgeb. Verfahren. 2020;**192**:754-763

[56] Kitajima K, Kihara T, Kawanaka Y, Kido A, Yoshida K, Mizumoto Y, et al. Neuroendocrine carcinoma of uterine cervix findings shown by MRI for staging and survival analysis – Japan multicenter study. Oncotarget. 2020;**11**:3675-3686

[57] Balleyguier C, Sala E, Da Cunha T, Bergman A, Brkljacic B, Danza F, et al. Staging of uterine cervical cancer with MRI: Guidelines of the European Society of Urogenital Radiology. European Radiology. 2011;**21**:1102-1110

[58] Wu Q, Wang S, Chen X, Wang Y, Dong L, Liu Z, et al. Radiomics analysis of magnetic resonance imaging improves diagnostic performance of lymph node metastasis in patients with cervical cancer. Radiotherapy and Oncology. 2019;**138**:141-148

[59] Ciolina M, Vinci V, Villani L, Gigli S, Saldari M, Panici PB, et al. Texture analysis versus conventional MRI prognostic factors in predicting tumor response to neoadjuvant chemotherapy in patients with locally advanced cancer of the uterine cervix. La Radiologia Medica. 2019;**124**:955-964

[60] Wang P, Thapa D, Wu G, Sun Q, Cai H, Tuo F. A study on diffusion and kurtosis features of cervical cancer based on non-Gaussian diffusion weighted model. Magnetic Resonance Imaging. 2018;**47**:60-66

[61] Wu Q, Shi D, Dou S, Shi L, Liu M, Dong L, et al. Radiomics analysis of multiparametric MRI evaluates the pathological features of cervical squamous cell carcinoma. Journal of Magnetic Resonance Imaging. 2019;**49**:1141-1148

[62] Becker AS, Ghafoor S, Marcon M, Perucho JA, Wurnig MC, Wagner MW, et al. MRI texture features may predict differentiation and nodal stage of cervical cancer: A pilot study. Acta Radiology. 2017;**6**:2058460117729574

[63] Duan X, Ban X, Zhang X, Hu H, Li G, Wang D, et al. MR imaging features and staging of neuroendocrine carcinomas of the uterine cervix with pathological correlations. European Radiology. 2016;**26**:4293-4302

[64] Miccò M, Vargas HA, Burger IA, Kollmeier MA, Goldman DA, Park KJ, et al. Combined pre-treatment MRI and 18F-FDG PET/CT parameters as prognostic biomarkers in patients with cervical cancer. European Journal of Radiology. 2014;**83**:1169-1176

[65] Downey K, Riches SF, Morgan VA, Giles SL, Attygalle AD, Ind TE, et al. Relationship between imaging biomarkers of stage I cervical cancer and poor-prognosis histologic features: Quantitative histogram analysis of diffusion-weighted MR images. American Journal of Roentgenology. 2013;**200**:314-320

[66] Vinh-Hung V, Bourgain C, Vlastos G, Cserni G, De Ridder M, Storme G, et al. Prognostic value of histopathology and trends in cervical cancer: A SEER population study. BMC Cancer. 2007;**7**:164

[67] Zhang X, Xu X, Tian Q, Li B, Wu Y, Yang Z, et al. Radiomics assessment of bladder cancer grade using texture features from diffusion-weighted imaging. Journal of Magnetic Resonance Imaging. 2017;**46**:1281-1288

[68] Cancer Grade Vs. Cancer Stage | MD Anderson Cancer Center, (n.d.)

[69] Odicino F, Pecorelli S, Zigliani L, Creasman WT. History of the FIGO cancer staging system. International Journal of Gynecology & Obstetrics. 2008;**101**:205-210

[70] Lee SI, Atri M. 2018 FIGO staging system for uterine cervical cancer: Enter cross-sectional imaging. Radiology. 2019;**292**:15-24

[71] Ai Y, Zhu H, Xie C, Jin X. Radiomics in cervical cancer: Current applications and future potential. Critical Reviews in Oncology/ Hematology. 2020;**152**:102985

[72] Lin Y, Li H, Chen Z, Ni P, Zhong Q, Huang H, et al. Correlation of histogram analysis of apparent diffusion coefficient with uterine cervical pathologic finding. American Journal of Roentgenology. 2015;**204**:1125-1131

[73] Guan Y, Li W, Jiang Z, Zhang B, Chen Y, Huang X, et al. Value of whole-lesion apparent diffusion coefficient (ADC) first-order statistics and texture features in clinical staging of cervical cancers. Clinical Radiology. 2017;**72**:951-958

[74] Scouse RA. Introduction to Statistical Quality Control. 1985

[75] Fiset S, Welch ML, Weiss J, Pintilie M, Conway JL, Milosevic M, et al. Repeatability and reproducibility of MRI-based radiomic features in cervical cancer. Radiotherapy and Oncology. 2019;**135**:107-114

[76] Baeßler B, Weiss K, Pinto dos Santos D. Robustness and reproducibility of radiomics in magnetic resonance imaging. Investigative Radiology. 2019;**54**:221-228

[77] Zwanenburg A, Vallières M, Abdalah MA, Aerts HJWL, Andrearczyk V, Apte A, et al. The image biomarker standardization initiative: Standardized quantitative radiomics for high-throughput image-based phenotyping. Radiology. 2020;**295**:328-338

[78] Jethanandani A, Lin TA, Volpe S, Elhalawani H, Mohamed ASR, Yang P, et al. Exploring applications of radiomics in magnetic resonance imaging of head and neck cancer: A systematic review. Frontiers in Oncology. 2018;**8**:131

[79] van Timmeren JE, Cester D, Tanadini-Lang S, Alkadhi H, Baessler B. Radiomics in medical imaging—"how-to" guide and critical reflection. Insights Imaging. 2020;**11**:91

[80] Avanzo M, Wei L, Stancanello J, Vallières M, Rao A, Morin O, et al. Machine and deep learning methods for radiomics. Medical Physics. 2020;**47**:e185-e202